# Direct monitoring of bicarbonate transport by emission spectroscopy

Luis Martínez-Crespo,[a] Sarah H. Hewitt,[b] Nicola Alessandro De Simone,[c] Vladimír Šindelář,[c] Anthony P. Davis,[d] Stephen Butler,[b] and Hennie Valkenier*[a]*

a. Université Libre de Bruxelles (ULB), Engineering of Molecular NanoSystems, Ecole polytechnique de Bruxelles, Avenue F.D. Roosevelt 50, CP165/64, B-1050 Brussels, Belgium. Hennie.Valkenier@ulb.ac.be
b. Loughborough University, Department of Chemistry, Epinal Way, Loughborough, LE11 3TU, United Kingdom. S.J.Butler@lboro.ac.uk
c. Masaryk University, Department of Chemistry and RECETOX, Faculty of Science, Kamenice 5, 625 00 Brno, Czech Republic.
d. University of Bristol, School of Chemistry, Cantock's Close, Bristol, BS8 1TS, United Kingdom.
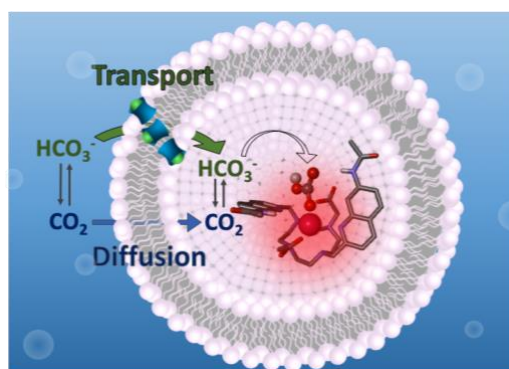
Abstract

The transmembrane transport of bicarbonate is a key step in many important biological processes, while problems with bicarbonate transport are at the origin of various diseases. Over the past 10 years, many anionophores that have been developed for the transport of chloride, have also been tested as bicarbonate transporters. However, methodology to directly monitor the kinetics of transport of bicarbonate is lacking, hence indirect methods have been used, which mainly rely on the monitoring of chloride concentrations.

Here we present an assay that allows the kinetics of bicarbonate transport into liposomes to be monitored directly, using emission spectroscopy. The assay utilises an encapsulated europium(III) complex, which exhibits a large increase in emission upon binding of bicarbonate. The advantages of this assay over existing methodology are that concentrations of bicarbonate are monitored directly and with a high sensitivity. This allows studies at very low concentrations of anionophores, and for the mechanisms of bicarbonate transport to be unravelled. We have distinguished classical antiport with bicarbonate from mechanisms involving CO_2 diffusion and the dissipation of a pH gradient. Furthermore, the use of a standard fluorescence spectrometer and liposomes with a diameter ~200 nm makes this assay readily and reliably applicable in many laboratories, where it can facilitate the development of bicarbonate transporters for applications in physiological studies or therapies.

Introduction

Transport of HCO_3^- across lipid bilayer membranes of living organisms is crucial for various processes, such as the regulation of pH[1] and the removal of metabolic waste.[2] A first example is found in red blood cells, which take up carbon dioxide that is excreted from cells in tissues as a waste product of aerobic respiration, and convert it into HCO_3^-. The bicarbonate transporter AE1 is an anion exchanging membrane protein that transports HCO_3^- out of the red blood cells, in exchange for Cl^-. This process prevents acidification of tissues and allows HCO_3^- to travel to the lungs in the blood stream. In the lungs the reverse processes will take place: HCO_3^- is transported into red blood cells (and Cl^- out) by AE1, after which the carbon dioxide diffuses from the red blood cells, to finally get exhaled.[2] Furthermore, HCO_3^-/Cl^- exchange by proteins from the SLC26 family and Cl^- and HCO_3^- transport by the channel CFTR play important roles in secretion of HCO_3^- and liquid into the lungs.[2,3] A second example is found in kidneys, where reabsorption of HCO_3^- takes place to avoid acidification of the organism. The HCO_3^-/Cl^- exchanger AE1 is present in certain parts of the tissue, while in other parts the protein NBCe1 performs symport of HCO_3^- and Na^+. The gastrointestinal tract provides a third example, as HCO_3^- is secreted to neutralise stomach acid. Furthermore, in the intestines the HCO_3^-/Cl^- exchange by proteins of the SLC26 family is coupled to H^+/Na^+ exchange by transport protein NHE3. This leads to the net reabsorption of NaCl, which in turn drives the reabsorption of water. These are only some examples of important biological processes that involve transmembrane transport of HCO_3^-.[2]

The importance of HCO_3^- transport is also demonstrated by diseases that are linked to mutations in HCO_3^- transporting proteins. Examples are haemolytic anaemia, renal diseases, congenital chloride diarrhoea, and glaucoma.[2] Altered expression patterns of HCO_3^- transporters have been observed in many types of cancer as well.[4] Many symptoms of the congenital disease *cystic fibrosis* (CF), primarily associated with deficient Cl^- transport, find their origin in a lack of HCO_3^- crossing epithelial cell membranes.[5,6,7]
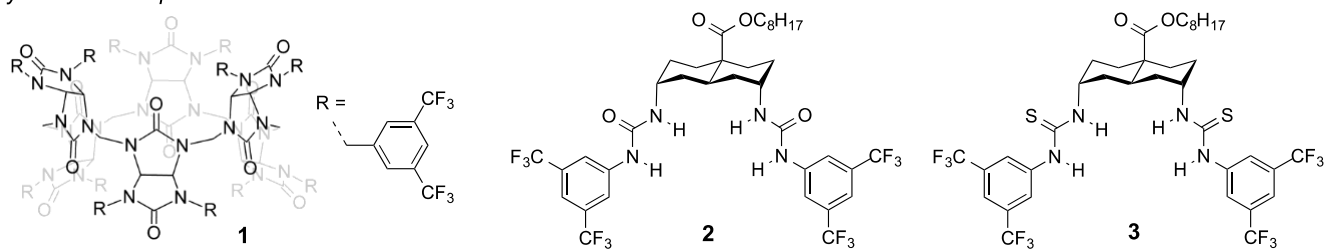
Supramolecular chemists have envisaged to perform the transport of HCO_3^- using synthetic anion receptors.[8,9] While the development of HCO_3^- transporters was defined as "an interesting target with potential utility" by A. P. Davis, Sheppard, and Smith in 2006,[10] J. T. Davis, Gale, Quesada and co-workers reported in 2009 that a series of isophthalamides and the natural compound prodigiosin can act as Cl^-/HCO_3^- exchangers.[11] Since then, many different anion transporters have been shown to transport HCO_3^-, of which the vast majority have urea,[12,13,14] thiourea,[15,16,17] squaramide,[18,19] amide,[11,20,21] or pyrrolic N-H groups[22,23] as H-bond donors. Phenyl rings with electron withdrawing substituents are often connected to these functional groups to increase the acidity of the N-H groups and improve both the affinity for anions and the rates of transport.[12-14,17-19] A series of compounds that was shown to function efficiently as Cl^-/HCO_3^- exchanging anionophores, but without employing N-H based H-bond donors, are the fluorinated bambus[6]urils.[24] These macrocyclic receptors have an electron deficient cavity formed by twelve (polarised) methine C-H groups, which leads to exceptionally high affinity constants in the range of 10^7-10^{11} M^{-1} in acetonitrile for HCO_3^-, Cl^-, and NO_3^-, despite the absence of acidic protons. Other anionophores employing C-H groups for anion recognition were, however, unable to transport HCO_3^-.[25,26]

In the context of CF, the strategy of employing relatively small synthetic molecules to achieve anion transport in epithelial cell membranes gave encouraging results for chloride transport by various compounds.[27,28,29,30,31,32] More recent results suggest that small synthetic anion carriers can transport HCO_3^- in cells as well.[33] The properties of airway surface liquid (ASL), which are linked to transport of HCO_3^-,[34] were restored significantly in CF airway epithelial tissue,[35] while the channel forming natural product amphotericin B, additionally, showed improvements in the ASL of CF pigs *in vivo*.[36]
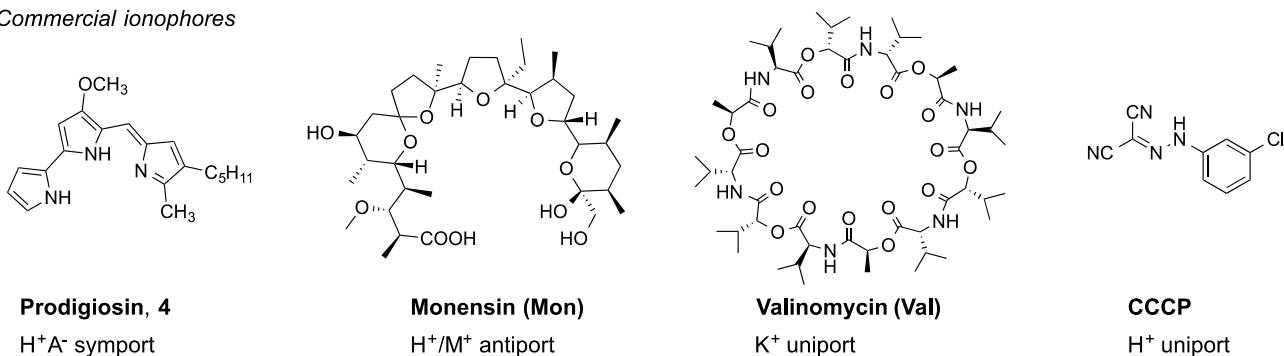
To further develop HCO$_3^-$ transporters for biological or therapeutic applications, direct and sensitive methods to study the transport of this anion would be of great benefit. So far, the ability of anionophores to transport HCO$_3^-$ has mainly been studied by indirect methods. In most cases, a chloride selective electrode has been employed to study the efflux of Cl$^-$ from liposomes that were dispersed in a medium containing HCO$_3^-$.[37,11,13-19,21-23,33] The transport of Cl$^-$ out of the liposomes proceeds only if another anion is transported in the opposite direction, to balance the charge by an antiport process. From the observed efflux of Cl$^-$ it is then concluded that an influx of HCO$_3^-$ has occurred. Alternatively, a halide-sensitive fluorescent probe, such as lucigenin or SPQ, is encapsulated in liposomes and the influx (or efflux) of Cl$^-$ is monitored via the quenching of the fluorescence.[12,20,24,25,38] This is again an indirect method to study the transport of HCO$_3^-$, which is assumed to balance the charge from the influx of Cl$^-$ if transport is observed. A third indirect method to monitor transport of HCO$_3^-$ is by the recently reported osmotic assay, where the efflux of HCO$_3^-$ by an anionophore is accompanied by the efflux of a cation (by a cationophore), resulting in an osmotic efflux of water, that can be observed as a change in the scattering intensity of the liposome dispersion.[17] To the best of our knowledge, the only reported alternative for these indirect methods to study the transmembrane transport of HCO$_3^-$ is the use of ^{13}C NMR spectroscopy, which can be employed in combination with NaH^{13}CO$_3$.[11,15,16,36,38] A paramagnetic species can be added after the influx (or efflux) of the isotopically labelled bicarbonate to distinguish interior from exterior bicarbonate. The disadvantage of this method is that it is difficult to monitor the transport process over time with standard instrument configurations.[36] Furthermore, the osmotic and ^{13}C NMR assays have a relatively low sensitivity and require large concentrations of transporter in the liposomes.

An emission-based assay that allows direct monitoring of HCO$_3^-$ transport would surmount these difficulties. Rates of HCO$_3^-$ transport could be quantified, and results obtained by indirect methods could be verified. It would also offer more possibilities to study the mechanism of transport and exchange processes with different anions. Such an assay requires a probe whose emission properties change in the presence of HCO$_3^-$. The europium complex [Eu.L^1]$^+$ developed by Butler (Fig. 1c) showed an increase in the intensity of several Eu(III) emission bands upon binding of HCO$_3^-$ but negligible responses to Cl$^-$ and NO$_3^-$ and this made it an ideal candidate for the development of the transport assay.[39] We present here the use of this probe encapsulated in liposomes, to directly monitor the transport of bicarbonate across the lipid bilayers by fluorescence spectroscopy. We have used this new assay to study the HCO$_3^-$ transport by different highly potent synthetic anionophores (Scheme 1),[12,24,40] for which transport was previous observed indirectly in the lucigenin assay (Fig. S1). Furthermore, this novel HCO$_3^-$ assay allowed the study of the kinetics and mechanisms of HCO$_3^-$ transport by these ionophores.

Synthetic anionophores

Commercial ionophores

Prodigiosin, 4

H^+A^- symport

Monensin (Mon)

H^+/M^+ antiport

Valinomycin (Val)

K^+ uniport

CCCP

H^+ uniport

Scheme 1 Structures of the different ionophores used in this study.

Results & Discussion

An emission assay to monitor transport of bicarbonate directly

The cationic Eu(III) complex [Eu.L^1]$^+$ (Fig. 1c) is based on a cyclen core possessing two pendant quinoline arms that absorb UV light around 330 nm, allowing efficient energy transfer to the central Eu(III) ion, which emits light in the visible range 570-720 nm. The Eu(III) probe has an open coordination site, occupied by a single water molecule in aqueous solution which quenches the Eu(III) emission significantly. In the presence of HCO$_3^-$, the coordinated water molecule is displaced upon binding of the hard oxyanion, resulting in a large enhancement in emission intensity (especially around 615 nm) and changes in spectral form (Fig. 1a).[39] The probe binds to the HCO$_3^-$ with high selectivity over poorly coordinating anions that are commonly used in anion transport assays, including Cl$^-$ and NO$_3^-$. The complex is also sensitive to hydroxide ions, and thus to pH, but this can be controlled with the help of a buffer as discussed later.

In order to use [Eu.L^1]$^+$ to monitor the transport of HCO$_3^-$, we encapsulated this probe into large unilamellar vesicles (LUVs) consisting of the POPC and cholesterol in a 7:3 ratio and extruded these liposomes through a membrane with 200 nm pores, to obtain LUVs with an average hydrodynamic diameter of 183 nm (Fig. S2). Liposomes of this diameter are routinely used for transport experiments by emission spectroscopy and can be prepared reliably with a high degree of unilamellarity, in contrast to much larger vesicles, as used in the ^{13}C NMR assay. An aqueous solution of 225 mM NaCl was used both interior and exterior to facilitate HCO$_3^-$/Cl$^-$ exchange (antiport) process and 5 mM HEPES buffer was added and adjusted to pH 7.0 (Fig. 1c). Anionophore **1** was preincorporated in the membrane of the LUVs and a NaHCO$_3$ solution was added to create a HCO$_3^-$ concentration gradient of 10 mM (Fig. S3). An increase in the intensity of the different emission bands of [Eu.L^1]$^+$ was observed (Fig. 1a) upon the addition of NaHCO$_3$. We chose to monitor the ΔJ = 2 emission band around 615 nm (see Fig. 1b), as this showed the strongest increase (Fig. 1a), in agreement with observations in titrations of [Eu.L^1]$^+$ with HCO$_3^-$.[39] From here on, we will refer to these experimental conditions as the EuL1 assay.
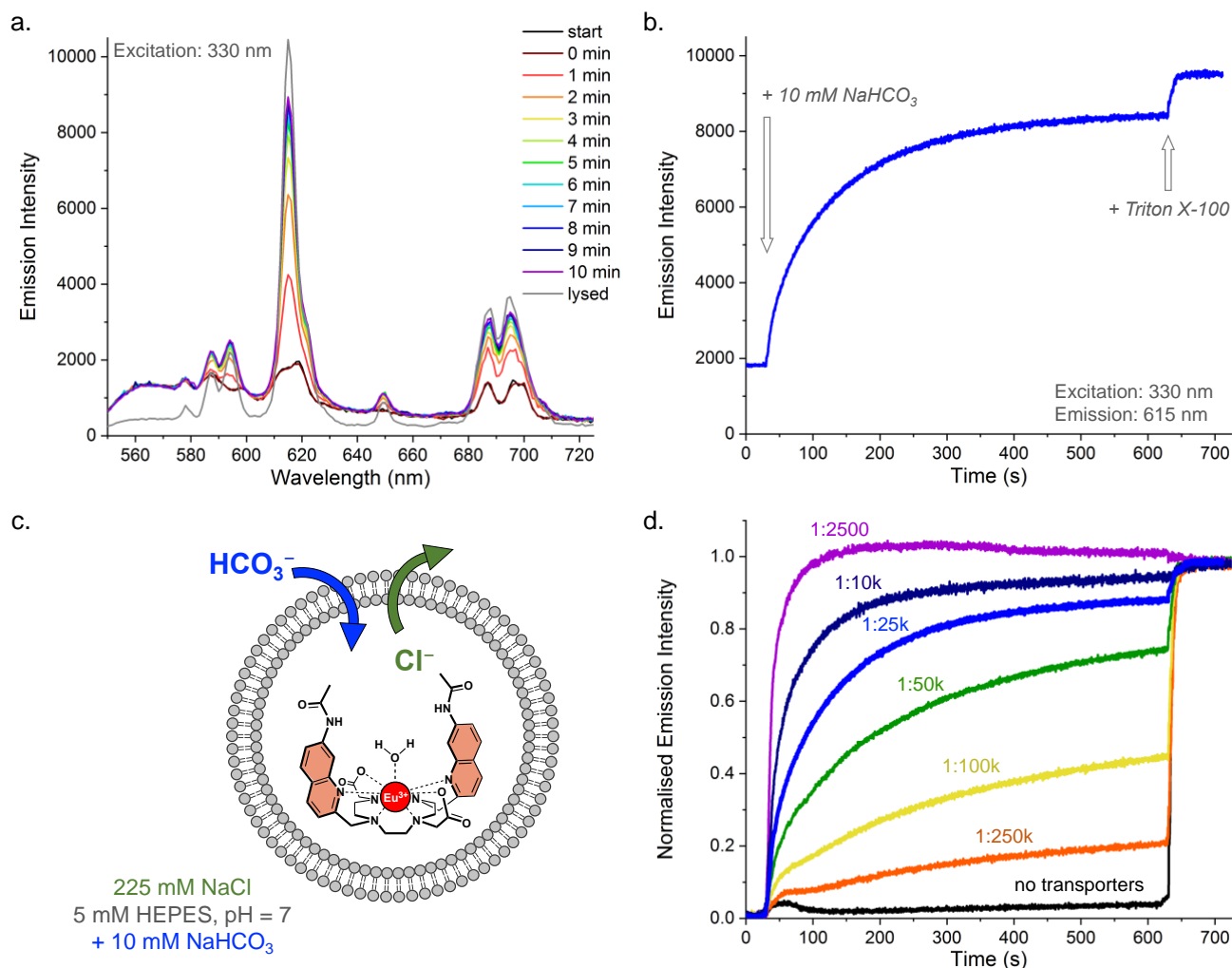
Fig. 1 Transport of HCO$_3^-$ by anionophore **1** preincorporated in LUVs with the probe [Eu.L^1]$^+$ encapsulated (50 μM), suspended in 225 mM NaCl with 5 mM HEPES at pH 7.0 (interior and exterior), upon addition of 10 mM NaHCO$_3$ after 30 seconds and lysis of the LUVs after 10 minutes. a. Emission spectra of [Eu.L^1]$^+$ recorded during the transport by **1** (at 1:25k transporter to lipid ratio); b. Emission intensity at 615 nm monitored over time for the transport as in a.; c. Schematic representation of EuL1 assay to study transport of HCO$_3^-$; d. Normalised transport curves for anionophore **1** preincorporated at various anionophore to lipid ratios.

The increase in the emission intensity over time upon the addition of NaHCO$_3$ indicates that HCO$_3^-$ has entered the liposomes. Since hardly any change in the emission intensity was observed in the absence of anionophore **1** (Fig. 1d, black curve), we can conclude that bambusuril **1** transports HCO$_3^-$ into the liposomes and that the new EuL1 assay allows to monitor this process.

The concentration of **1** that was preincorporated into the liposomes was varied from one bambusuril per 250,000 lipids (Fig. 1d, orange curve) to one per 2500 lipids (Fig. 1d, purple curve) and a clear increase in the rate of transport was observed for increasing concentrations of anionophore **1**. This shows that the EuL1 assay is highly sensitive and can be used to study the kinetics of HCO$_3^-$ transport. Furthermore, these results reinforce our previous findings that bambusuril **1** is a very potent HCO$_3^-$/Cl$^-$ transporter,[24] showing activity at 1:250k ratio, which corresponds to an average of two bambusurils per LUV.

Apparent transport of bicarbonate by cationophores

During our initial experiments to develop the EuL1 assay to study the transport of bicarbonate, we noticed that not only liposomes with anionophores gave an increase in emission intensity, but that also the addition of monensin to the LUVs gave a clear response (Fig. 2, red curve). Furthermore, we noticed that monensin also gives a positive response in the ^{13}C NMR assay for HCO_3^-/Cl^- transport (see ESI Section 4).[11] Monensin is a well-known cationophore,[41,42,43] that can wrap around cations, using its O atoms to interact.[44] It is not likely that this compound, nor its complex with Na^+ or K^+, can bind bicarbonate sufficiently strongly to cause transport. Valinomycin, another well know cationophore, was also tested in the EuL1 assay, but showed a much smaller response (Fig. 2, blue curve), indicating that $M^+HCO_3^-$ ion pairs are not readily transported by cationophores, as expected.
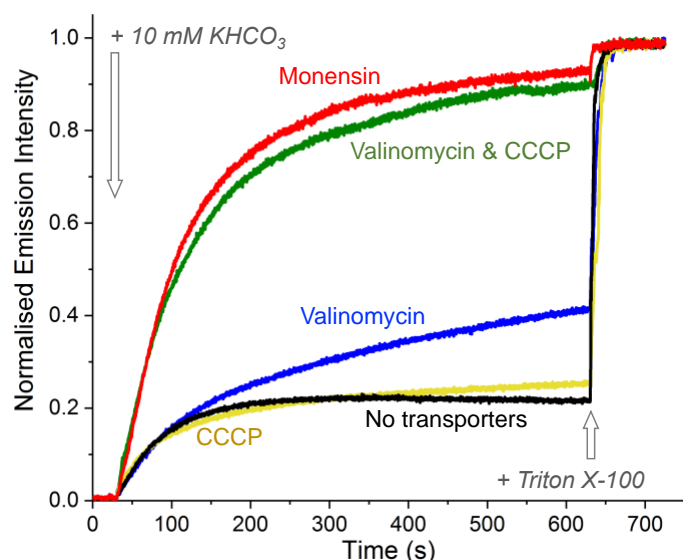

Fig. 2 Transport as monitored by the EuL1 assay in 112 mM K_2SO_4 with 5 mM HEPES at pH 7, upon addition of 10 mM $KHCO_3$ after 30 seconds. Different cation transporters were added to the LUVs at a transporter to lipid ratio of 1:1000.

However, when studying the transport of HCO_3^-, we should take into account that addition of a pulse of $MHCO_3$ to the exterior of the liposomes does not only create a gradient of HCO_3^-, but also of its conjugate acid H_2CO_3 [17] and of CO_2, formed upon dehydration.[45] We should note that at equilibrium the concentration of CO_2 is almost 1000-fold higher than that of H_2CO_3 in aqueous salt solutions.[46] Furthermore, it is well known that CO_2 can diffuse spontaneously across the membranes of cells which play important roles in HCO_3^- homeostasis,[47] such as red blood cells and renal epithelial cells.[2]

$$HCO_3^- + H^+ \rightleftharpoons H_2CO_3$$
$$\rightleftharpoons \qquad \rightleftharpoons$$
$$CO_2 + H_2O$$
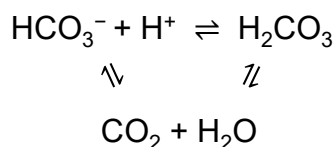
We should thus consider the possibility that CO_2 diffuses across the membranes of our liposomes, upon the addition of the $MHCO_3$ pulse. This increase of the concentration of CO_2 inside the liposomes would result in an acidification of the interior, causing a pH gradient to build up, which will stop the diffusion of CO_2. However, in the presence of an ionophore which can transport protons to prevent the build-up of a pH gradient, the diffusion of CO_2 can continue until the CO_2 gradient has been dissipated. Inside the liposomes, the diffused CO_2 will establish equilibria with its hydrate H_2CO_3 and the deprotonated form HCO_3^-. The formation of this bicarbonate anion is observed as a positive luminescence response of the EuL1 assay (Fig. 2, red curve). Thus, the diffusion of CO_2 into the LUVs (giving H_2CO_3) combined with ionophore facilitated transport of H^+ out of the LUVs, results in a net transport of HCO_3^-.

When studying transmembrane transport processes in LUVs, transport of charges should be balanced to avoid an electric potential from building up. Transport of HCO_3^- into LUVs can be balanced by transport of another anion out of the LUVs (Fig. 3, mechanism A). When CO_2 diffuses into LUVs and acidification is prevented by transport of protons out of the LUVs, this charge transport has to be balanced by either the transport of cations into the LUVs (Fig. 3, mechanism B) or transport of anions out of the LUVs (Fig 3, mechanism C). Alternatively, acidification by CO_2 diffusion can be prevented by hydroxide transport into the LUVs, balanced by transport of other anions out of the LUVs (Fig 3, mechanism D), which can often not be distinguished from mechanism C.
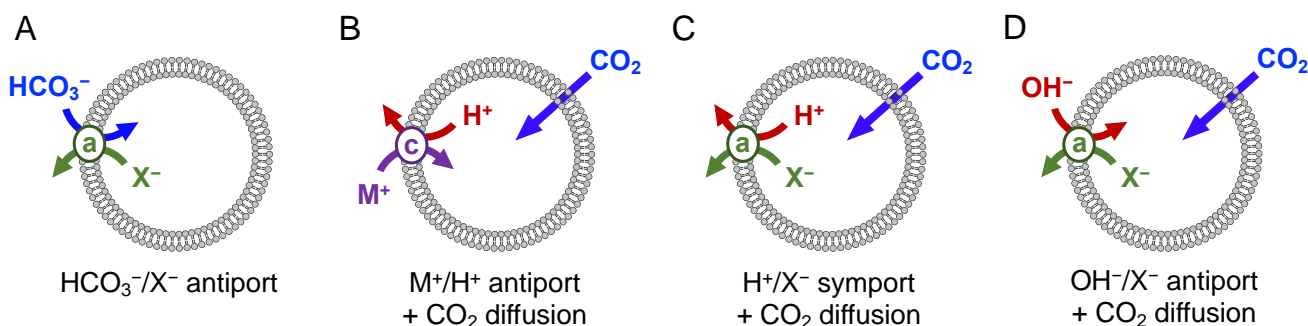

Fig. 3 Different mechanisms by which apparent transport of HCO_3^- could occur. In mechanism A, anionophore (a) exchanges HCO_3^- for another anion. Mechanisms B-D rely on the diffusion of CO_2 coupled to transport of H^+ or OH^- by cationophores (c) or anionophores to result in the net transport of HCO_3^-, without this anion crossing the membrane.

Monensin is well known to efficiently exchange protons with Na^+ or K^+ cations (H^+/M^+ antiport),[41] dissipating pH gradients and thus compensating for CO_2 diffusion, resulting in the apparent transport of HCO_3^- that the red curve in Fig. 2 indicates, following mechanism B. In contrast, valinomycin performs electrogenic transport of K^+, but is not capable of transporting protons via H^+/M^+ antiport,[48] thus preventing diffusion of CO_2. The protonophore carbonyl cyanide 3-chlorophenylhydrazone (CCCP) is known to transport protons, but no other cations.[49] Adding CCCP to the EuL1 assay did not result in a response (Fig. 2, yellow curve), but adding both valinomycin and CCCP to the LUVs in K_2SO_4 solution gave apparent HCO_3^- transport with similar rates as monensin (Fig. 2, green curve), via a similar mechanism. In this case, the acidification by CO_2 diffusion is prevented by CCCP transporting protons out of the LUVs, while valinomycin transports K^+ into the LUVs for charge balance. Also, the ion channel gramicidin, which is capable of transporting various cations, including H^+, Na^+, and K^+, can give apparent HCO_3^- transport via mechanism B (Fig. S4).

To confirm that the apparent transport of HCO_3^- by monensin[17] as observed in the EuL1 assay is indeed caused by mechanism B, the conditions of the assay were varied. Neither the CO_2 diffusion nor the H^+/M^+ antiport would involve the anion X^-, thus variations of the anion would not be expected to significantly impact the rate of apparent HCO_3^- transport. Indeed, monensin gives similar transport curves in MCl, MNO_3, and M_2SO_4 solutions (where M^+ is Na^+ or K^+, see Fig. S5 and 4a). No systematic differences were observed between the experiments in sodium and in potassium salts. This could mean either that monensin performs H^+/Na^+ and H^+/K^+ antiport at identical rates, or that the formation[45] and diffusion of CO_2 are rate limiting in mechanism B. To distinguish between these options, we varied the concentration of monensin. While decreasing the monensin to lipid ratio from 1:1000 to 1:10,000 gave a lower rate of transport, increasing to a ratio of 1:100 did not significantly impact the rate of transport (Fig. S6). This confirms that the diffusion of CO_2 is rate limiting in the apparent transport of HCO_3^- and not the H^+/M^+ antiport by monensin.

Considering that the role of monensin in the proposed transport process is to prevent the formation of a pH gradient upon CO_2 diffusion, we may expect that in the absence of any transporters the concentration of the buffer and the pH at which the experiments are performed determine how much

CO$_2$ can diffuse into the LUVs before the pH gradient stops this process. When controls for transport experiments were performed by adding 10 mM NaHCO$_3$ to LUVs in 20 mM HEPES at a starting pH of 7.6, the external pH increased to 7.7 and a much larger apparent influx of HCO$_3^-$ was observed (Fig. S7) than when working with 5 mM HEPES at pH 7.0 (where addition of 10 mM NaHCO$_3$ increases the pH to 7.4). HEPES has a pK$_a$ of 7.5 and the optimal buffer range is reported to be 6.8-8.2,[50] thus the higher concentration of HEPES can compensate the effect of the acidification by CO$_2$ influx. When 20 mM HEPES was used but starting at pH 6.5, the buffer could not compensate for the acidification and hardly any CO$_2$ diffusion was observed (Fig. S8).

To verify if the pH inside the LUVs changes as expected upon diffusion of CO$_2$ (in absence of ionophores) or upon dissipation of the pH gradient by monensin, transport experiments were performed in which the pH sensitive probe HPTS was encapsulated instead of the bicarbonate sensitive probe [Eu.L^1]$^+$. All other conditions were identical to those used in the EuL1 assay (*i.e.*, 225 mM NaCl, 5 mM HEPES, pH 7.0). The results in Fig. 4d indeed show that the addition of 10 mM NaHCO$_3$ to LUVs with monensin (1:1000 ratio) results in a rapid increase of the pH (red curve), indicating the equilibration of the pH gradient caused by the addition of the basic solution of NaHCO$_3$. In contrast, addition of NaHCO$_3$ to LUVs without transporters results in an acidification of the interior (black curve), in agreement with the formation of carbonic acid upon diffusion of CO$_2$. LUVs with a very low concentration of monensin (1:50k) show an initial acidification of the interior due to CO$_2$ diffusion, followed by a slow increase of the pH due to the H$^+$/Na$^+$ antiport by monensin. These experiments with HPTS thus confirm that the apparent transport of HCO$_3^-$ by monensin can be attributed to mechanism B, permitted by dissipation of the pH gradient. Furthermore, these data show that the pH equilibration by monensin at 1:1000 ratio (Fig. 4d) is much faster than the apparent HCO$_3^-$ transport revealed by the EuL1 assay (Fig. 4a), which is further proof that CO$_2$ diffusion (and/or formation[45]) is rate limiting in the net transport of HCO$_3^-$ by monensin (at 1:1000 ratio).
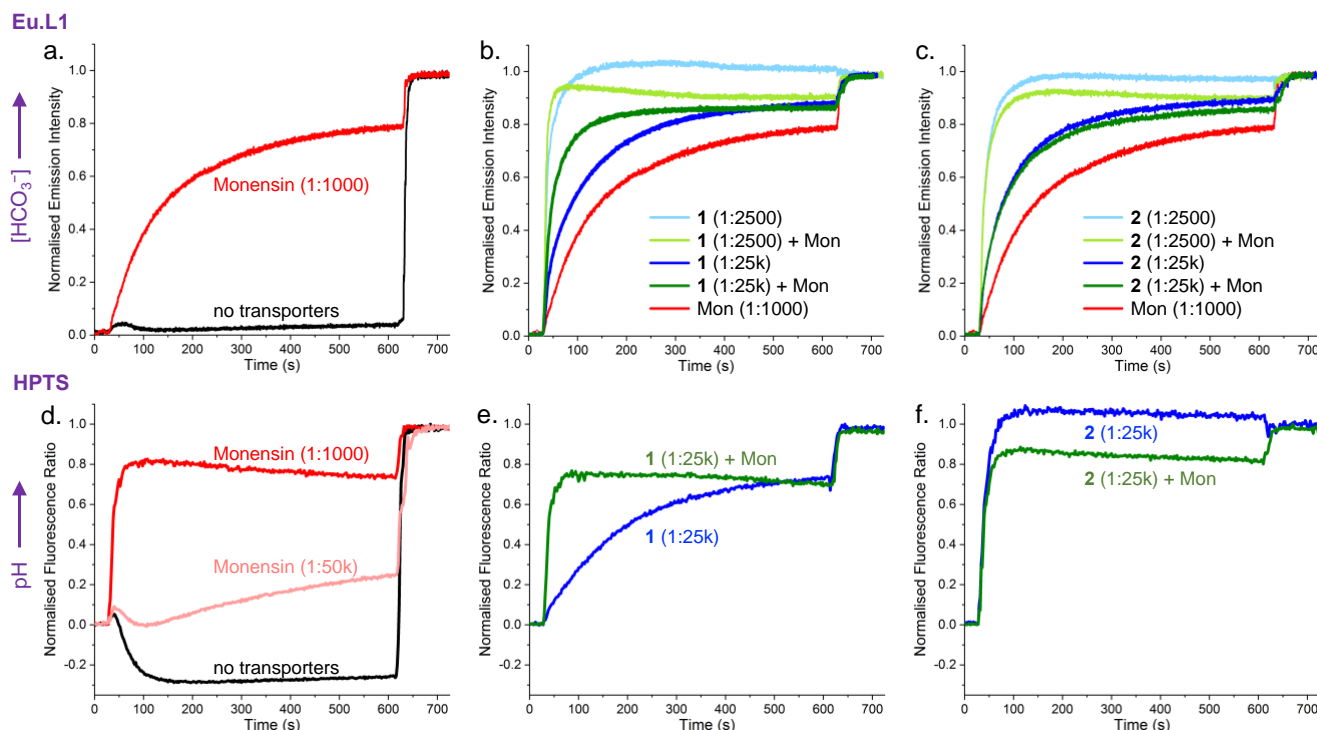

Fig. 4 Transport by monensin (a,d), bambusurils **1** (b,e) and urea **2** (c,f) as monitored by the EuL1 assay (a-c) or by the pH sensitive probe HPTS (d-f) in 225 mM NaCl with 5 mM HEPES at pH 7, upon addition of 10 mM NaHCO$_3$ after 30 seconds and lysis of the LUVs 10 minutes after that. Monensin (1:1000 transporter to lipid ratio) was added to the experiments with anionophores **1** and **2**.

Analysis of the transport mechanisms by the different anionophores

Following experiments with bambusuril **1** and the various cationophores, we have studied the transport by anionophores **2-4** in the EuL1 assay in NaCl (blue curves in Fig. 4c and S9). A clear increase of the emission intensity was observed for all anionophores, even at the relatively low concentration of 1:25,000 (transporter to lipid ratio), indicating efficient HCO_3^- transport.

However, having observed that monensin and other cation transporters capable of dissipating pH gradients can show apparent HCO_3^- transport in the EuL1 assay, without actually transporting the HCO_3^- anion, we have to consider if the observed transport by anionophores **1-4** is caused by HCO_3^-/Cl^- antiport (mechanism A), or whether other mechanisms could give a similar response. Gale and co-workers have clearly demonstrated that many urea and thiourea based receptors not only transport anions such as Cl^- (and NO_3^-), but are also capable of dissipating pH gradients via H^+Cl^- symport or OH^-/Cl^- antiport processes (which can generally not be distinguished).[51] These processes would prevent acidification of the interior of LUVs upon diffusion of CO_2, as shown in Fig. 3 mechanisms C and D. This implies that anionophores could show apparent HCO_3^- transport that originates from CO_2 diffusion and proton or hydroxide transport, in a similar way as observed for monensin.

To distinguish between the HCO_3^-/Cl^- antiport mechanism A versus the pH equilibration mechanisms C and D, we should firstly consider if anionophores are capable of performing H^+Cl^- symport or OH^-/Cl^- antiport. Bambusuril **1** cannot be readily protonated nor deprotonated, processes that would favour H^+ transport. We have previously shown that bambusuril **1** is indeed not able to dissipate pH gradients in the presence of Cl^- or NO_3^-, and thus is incapable of H^+Cl^- symport and OH^-/Cl^- antiport.[24] Indeed, when monitoring the pH changes inside the liposomes with bambusuril **1** upon addition of $NaHCO_3$ (blue curve in Fig. 4e), a gradual increases in pH is observed, resembling the kinetics of the transport of the basic HCO_3^- anion into the LUVs (blue curve in Fig. 4b). Having excluded mechanisms C and D, we can conclude that the transport observed by bambusuril **1** takes place via HCO_3^-/Cl^- antiport (mechanism A).

In contrast to bambusuril **1**, prodigiosin **4** is a well-known HCl transporter, as the pyrrole ring is readily protonated.[52,53] Decalin bis-urea **2** and bis-thiourea **3** both have phenyl rings with electron withdrawing substituents, resulting in relatively acidic (thio)urea N-H groups, making them good candidates for HCl symport or OH^-/Cl^- antiport.[51] When monitoring the pH inside the LUVs with compounds **2-4** upon addition of $NaHCO_3$, a rapid equilibration of pH was observed (Fig. 4f and S18, blue curves). This pH equilibration is much faster than the response by the same concentration of these compounds in the EuL1 assay (Fig. 4c and S9), resembling the effect by monensin (Fig. 4d). This demonstrates that compounds **2-4** indeed perform HCl symport or OH^-/Cl^- antiport efficiently and that apparent HCO_3^- transport by mechanisms C or D could take place.

To study if mechanisms C or D indeed take place, we have performed transport experiments in which we added monensin to LUVs with the anionophores (Fig. 4 and S9-11, green curves). For bambusuril **1**, addition of monensin gives a clear increase in the rate of transport as seen from the comparison of the green to the blue curves in Fig 4b and S11. This increase can be understood from the combined effect of mechanism A by **1** and mechanism B by monensin, leading to a higher rate of net transport of HCO_3^- than by either of these two processes alone. In contrast, addition of monensin to LUVs with anionophores **2-4** did not increase the rate of transport, as shown for **2** in Fig. 4c and for **3-4** in Fig. S11. We have seen that pH equilibration by these compounds is nearly instantaneous when incorporated at 1:25,000 transporter to lipid concentration, thus that CO_2 diffusion would most likely be rate-limiting in mechanisms C and D, as it was for monensin in mechanism B (see above). If CO_2 diffusion is rate-limiting in the transport by **2-4** via mechanisms C and D, the addition of monensin will not have any impact on the overall rate of (apparent) HCO_3^- transport, as this will remain limited by CO_2 diffusion. Thus, the fact that addition of monensin does not change the rate of transport by **2-4** does mean that these anionophores act via mechanism C or D.

This brings us to question whether these compounds perform any HCO_3^-/Cl^- transport (mechanism A) in addition to their transport by mechanisms C and D. To test this, we have increased the concentrations of **2** and **3** that were preincorporated in the membranes of the liposomes to 1:2500 (transporter to lipid ratio). The light blue curves in Fig. 4c and S9a show that this ten-fold increase in transporter concentration indeed leads to a significantly faster rate of (apparent) HCO_3^- transport, and that this overall rate clearly exceeds rates of transport that are limited by CO_2 diffusion (as observed in the curves for monensin ≥ 1:1000 ratio, see also Fig. S10). From this we can conclude that the transport observed by compounds **2** and **3** in the EuL1 assay results from the combination of HCO_3^-/Cl^- antiport mechanism A with CO_2 diffusion mechanism C or D. These compounds dissipate the pH gradient faster than they transport HCO_3^- and as a result C or D is the main mechanism, up to the point that CO_2 diffusion becomes rate limiting, after which mechanism A contributes to the net HCO_3^- transport.

Table 1 Performance of anionophores **1**-**3** and prodigiosin in the EuL1 assay in NaCl and $NaNO_3$.

Salt	Aniono-phore	Concentration	Transport (without monensin)		Transport (with monensin)[c]	
		(anionophore:lipid)	Half-life (s)[a]	Initial rate (s⁻¹)[b]	Half-life (s)[a]	Initial rate (s⁻¹)[b]
NaCl	None		*	*	82	0.008
	1	1:2500	10	0.124	4	0.178
		1:10k	32	0.041	17	0.059
		1:25k	64	0.026	21	0.051
		1:50k	110	0.015	40	0.025
		1:100k	*	*	58	0.015
		1:250k	*	*	83	0.009
	2	1:2500	12	0.093	11	0.091
		1:25k	51	0.019	50	0.017
	3	1:2500	12	0.077	11	0.071
		1:25k	46	0.021	47	0.020
	4	1:25k	59	0.012	74	0.012
$NaNO_3$	None		*	*	81	0.008
	1	1:2500	*	*	67	0.009
		1:25k	*	*	85	0.007
	2	1:2500	45	0.021	40	0.022
		1:25k	89	0.007	85	0.007
	3	1:2500	16	0.060	14	0.052
		1:25k	65	0.014	59	0.013
	4	1:25k	61	0.012	68	0.011

[a] Calculated from a single exponential fit of the transport curve, see ESI for details.
[b] Calculated from a double exponential fit of the transport curve, see ESI for details.
[c] Transport in presence of monensin at a 1:1000 monensin to lipid ratio.
* Transport was absent or too slow to quantify.

Quantitative comparison of rates of transport

To verify the qualitative trends and comparisons described above, we have fitted the transport data from the EuL1 assay with single and double exponential functions, to obtain half-lives and initial rates respectively (see ESI for details). The results are summarised in Table 1. In NaCl solutions, the half-lives of transport by bambusuril **1** clearly decrease by a factor two or more when monensin is present (see also Fig. S12). In contrast, the half-lives by **2**-**4** are nearly identical. Similar trends are observed when comparing the initial rates.

When comparing initial rates of transport as measured in the EuL1 assay quantitively, we should consider the effect of the different pH profiles during the transport measurements (Fig. 4d-f), as the $[Eu.L^1]^+$ probe is not only sensitive to concentrations of HCO_3^-, but also to pH.[39] While the effects of pH on the emission intensity were reported to be small at pH ≤ 8,[39] the pH has a more noticeable effect on the increase of luminescence observed upon addition of HCO_3^-. The titrations in Fig. S13-14 show that this increase of emission intensity is larger at pH 7.4 than at pH 7.0, leading to different apparent affinities of EuL1 for HCO_3^-. In the presence of monensin, the pH rapidly equilibrates to ~7.4 (Fig. 4e, green curve), thus resulting in a higher sensitivity of the probe to HCO_3^-, which could result in a higher apparent initial rate compared to transport measured under conditions without pH equilibration (*i.e.*, with only **1** present in the LUVs).

Based on the discussion of the additivity of mechanisms A and B, we could have expected that initial rates of transport by **1** (at different concentrations) and by monensin alone (1:1000 ratio) could be added to predict the initial rates of transport by the combination of **1** and monensin. However, in Table 1 we see that the values found are higher than those predicted by this hypothesis, especially at higher concentrations of **1** (≥ 1:25k ratio). This could be explained by the effects of the pH on the initial rates, as discussed above. Furthermore, the normalisation of the data could result in an error on the values of the initial rates, but not the half-lives. Therefore, half-lives are more reliable to compare transport data of **1** in presence and absence of monensin, as these values indicate how fast equilibrium is reached, independent of absolute emission values. The comparison of half-lives of transport by **1** with and without monensin clearly shows that equilibrium is reached much faster in the presence of monensin (Table 1 and Fig. S12), confirming the additivity of mechanisms A and B.

Table 1 also shows that the overall rates of apparent HCO_3^- transport by anionophores **1**-**4** (in absence of monensin) are rather similar. However, the different pH profiles will affect this comparison and it would thus be better to compare the different transporters in the presence of monensin. Under those conditions, CO_2 diffusion based mechanisms contribute to the transport for all the compounds, but as this process has a limited and thus constant rate, the differences in half-lives and initial rates between anionophores **1**-**4** (in presence of monensin) can be attributed to the difference in rates of HCO_3^-/Cl^- antiport by the anionophores. In this comparison, bambusuril **1** is clearly the most active ionophore for HCO_3^-/Cl^- antiport. Bis-urea **2** and bis-thiourea **3** show similar rates of transport and are slightly more active than prodigiosin **4**, for which the half-life is very close to that of transport by monensin alone.

Bicarbonate transport experiments in NaNO₃

The newly developed EuL1 assay does not only allow the study of HCO_3^-/Cl^- exchange, but can also be used to study the exchange of bicarbonate with other anions, such as nitrate. Commonly employed indirect methods to study HCO_3^- transport rely on the monitoring of Cl^- concentrations and could thus not be used to study the exchange between HCO_3^- and NO_3^-, while $[Eu.L^1]^+$ does not bind to either Cl^- or NO_3^- and could thus be used to monitor HCO_3^-/NO_3^- exchange in the same way as HCO_3^-/Cl^- exchange.[39] Fig. 5 shows the transport curves by anionophores **1**-**4** at 1:25,000 ratio in the EuL1 assay in NaNO₃, and the curve of monensin (1:1000) is included for comparison. Results from experiments at different concentrations of ionophores, both in presence and absence of monensin, are included in Table 1 and Fig. S16.
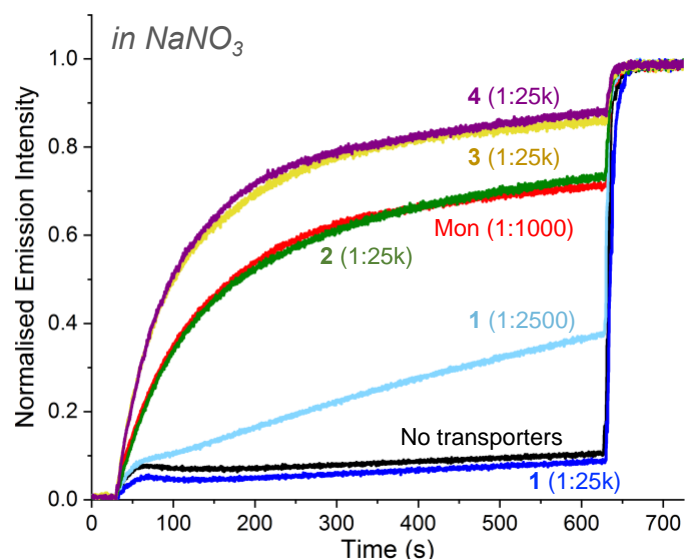
Fig. 5 Transport by anionophores **1-4** and monensin, as monitored by the EuL1 assay in 225 mM NaNO$_3$ with 5 mM HEPES at pH 7, upon addition of 10 mM NaHCO$_3$ after 30 seconds and lysis of the LUVs after 10 minutes.

Compounds **2-4** show efficient (apparent) transport of HCO$_3^-$ in NaNO$_3$ and rates do not change upon addition of monensin, similar to the results obtained for these compounds in NaCl, indicating that the same combination of mechanisms applies. We note, however, that the overall HCO$_3^-$ transport by **2** and **3** is somewhat less efficient in NaNO$_3$ than in NaCl, and that this difference is more pronounced for urea **2** than for thiourea **3**. Gale *et al.* have reported that anionophores can display selectivity in transport for either Cl$^-$ or NO$_3^-$ and that this selectivity can be correlated to the relative affinities for these anions.[54] They found that compounds with the highest affinities were clearly more selective for Cl$^-$ over NO$_3^-$, both in binding and transport.[55] It is thus not unsurprising that compounds **2** and **3**, both efficient receptors for Cl$^-$, could transport Cl$^-$ more easily than NO$_3^-$, resulting in higher rates of (apparent) HCO$_3^-$ transport in NaCl than in NaNO$_3$.

In contrast to anionophores **2-4**, bambusuril **1** showed no transport at a 1:25,000 ratio, and only very slow transport was observed when using a 10-fold higher concentration of **1** (1:2500, Fig. 5 light blue curve). This slow HCO$_3^-$/NO$_3^-$ exchange by **1** resembles the results reported for Cl$^-$/NO$_3^-$ exchange, which was found to be 100-fold slower than Cl$^-$/HCO$_3^-$ exchange by this bambusuril.[24] We proposed that this large difference in rates of Cl$^-$ transport by **1** could be explained by a combination of two phenomena. Firstly, the very high affinity of **1** for NO$_3^-$ ($K_a = 5 \times 10^{11}$ M^{-1} in acetonitrile) could prevent the release of this anion. Secondly, we postulated that the simultaneous binding of a Cl$^-$ and a HCO$_3^-$ anion in the bambusuril could facilitate the exchange of these anions.[24] Even though the formation of an equivalent complex with NO$_3^-$ and HCO$_3^-$ simultaneously is possible, this does not appear to increase the rate of the exchange of these two anions. Instead, the very strong binding of NO$_3^-$ is the most likely explanation for the low rates of HCO$_3^-$/NO$_3^-$ exchange by **1** (see also Fig. S17).

Thus, when comparing the rates of apparent transport of HCO$_3^-$ in NaNO$_3$, thiourea **3** and prodigiosin **4** are the most efficient anionophores, followed closely by urea **2**, while bambusuril **1** is clearly the least efficient transporter under these conditions.

Conclusions

The results presented above demonstrate a new emission assay to directly monitor transport of HCO_3^- into liposomes, using the encapsulated europium complex $[Eu.L^1]^+$, of which the luminescence increases upon binding HCO_3^-. This assay is highly sensitive and thus permits the use of low concentrations of anionophores, comparable to fluorescence-based assays that are used to monitor the influx of Cl^-, which facilitates comparisons between anionophores.[24]

An important advantage of this direct and highly sensitive EuL1 assay is that it allows the study of the mechanisms involved in the transmembrane transport of HCO_3^-. We have revealed that the diffusion of CO_2 coupled to protonophoric activity can result in apparent (or net) transport of HCO_3^-. By this mechanism, the cationophore monensin appears to be able to act as a net transporter of HCO_3^-, in agreement with previous observation by Gale *et al*[17] and our results with ^{13}C NMR assay (Fig. S19).

Further analysis of transport data by anionophores **1**-**3** at different concentrations and in combination with monensin, permitted to unravel the mechanisms of the transport observed in the EuL1 assay. We confirmed that bambusuril **1** exclusively acts as HCO_3^-/Cl^- antiporter, which in combination with the high rates of transport achieved, highlights that this is a promising anionophore for biological applications, provided that it can be delivered to cells.

However, urea **2** and thiourea **3** combine a mechanism that involves CO_2 diffusion and the dissipation of a pH gradient with HCO_3^-/Cl^- antiport. These results lead us to consider the possibility that other anionophores which have been reported as HCO_3^- transporters, and that are able to transport either H^+ or OH^-,[51] might primarily rely on CO_2 diffusion instead of HCO_3^- transport. Only for very potent anion transporters, for which the rate of total apparent HCO_3^- transport surpasses the limiting rate of CO_2 diffusion, can we conclude with certainty that these act as anionophores for HCO_3^-.

The EuL1 assay also allowed, for the first time, to study the kinetics of HCO_3^-/NO_3^- exchange. This revealed that thiourea **3** and urea **2** are efficient transporters for this process, while bambusuril **1** performed very poorly, similar to previous observations for Cl^-/NO_3^- transport by this macrocycle.[24] Furthermore, it is possible to modulate the anion binding and sensing properties of this class of Eu(III) probes through modifications in the ligand structure,[56] auguring well for monitoring the transport of other anions using the strategy developed herein.

We are convinced that the new opportunities provided by this assay to study transport of HCO_3^- efficiently and in great detail can contribute to the further development of HCO_3^- transporters for biomedical purposes, such as channel replacement therapies.[10,57] The assay developed in this work will also inform the future design of Eu(III) probes capable of monitoring spatio-temporal HCO_3^- dynamics within living cells. Indeed, a derivative of $[Eu.L^1]^+$ has already been shown to permeate living cells and localise to specific subcellular compartments.[58]

Acknowledgements

References

[1] M. Tresguerres, J. Buck and L. R. Levin, *Pflugers Arch. - Eur. J. Physiol.*, 2010, **460**, 953–964.

[2] E. Cordat and J. R. Casey, *Biochem. J.*, 2009, **417**, 423–439.

[3] J. P. Garnett, E. Hickman, R. Burrows, P. Hegyi, L. Tiszlavicz, A. W. Cuthbert, P. Fong and M. A. Gray, *J. Biol. Chem.*, 2011, **286**, 41069–41082.

[4] A. Gorbatenko, C. W. Olesen, E. P. Boedtkjer and S. F. P. Pedersen, *Front. Physiol.*, 2014, **5**, 130.

[5] J. Y. Choi, D. Muallem, K. Kiselyov, M. G. Lee, P. J. Thomas and S. Muallem, *Nature*, 2001, **410**, 94–97.

[6] M. J. Hug, T. Tamada and R. J. Bridges, *News Physiol. Sci.*, 2003, **18**, 38–42.

[7] K. Kunzelmann, R. Schreiber and H. B. Hadorn, *J. Cystic Fibrosis*, 2017, **16**, 653–662.

[8] P. A. Gale, J. T. Davis and R. Quesada, *Chem. Soc. Rev.*, 2017, **46**, 2497–2519.

[9] H. Valkenier and A. P. Davis, *Acc. Chem. Res.*, 2013, **46**, 2898–2909.

[10] A. P. Davis, D. N. Sheppard and B. D. Smith, *Chem. Soc. Rev.*, 2007, **36**, 348–357.

[11] J. T. Davis, P. A. Gale, O. A. Okunola, P. Prados, J. C. Iglesias-Sánchez, T. Torroba and R. Quesada, *Nat. Chem.*, 2009, **1**, 138–144.

[12] S. Hussain, P. R. Brotherhood, L. W. Judd and A. P. Davis, *J. Am. Chem. Soc.*, 2011, **133**, 1614–1617.

[13] L. E. Karagiannidis, C. J. E. Haynes, K. J. Holder, I. L. Kirby, S. J. Moore, N. J. Wells and P. A. Gale, *Chem. Commun.*, 2014, **50**, 12050–12053.

[14] M. Olivari, R. Montis, S. N. Berry, L. E. Karagiannidis, S. J. Coles, P. N. Horton, L. K. Mapp, P. A. Gale and C. Caltagirone, *Dalton Trans.*, 2016, **45**, 11892–11897.

[15] N. Busschaert, P. A. Gale, C. J. E. Haynes, M. E. Light, S. J. Moore, C. C. Tong, J. T. Davis and J. William A. Harrell, *Chem. Commun.*, 2010, **46**, 6252–6254.

[16] N. J. Andrews, C. J. E. Haynes, M. E. Light, S. J. Moore, C. C. Tong, J. T. Davis, W. A. Harrell Jr and P. A. Gale, *Chem. Sci.*, 2011, **2**, 256–260.

[17] L. A. Jowett, E. N. W. Howe, X. Wu, N. Busschaert and P. A. Gale, *Chem. Eur. J.*, 2018, **24**, 10475–10487.

[18] N. Busschaert, I. L. Kirby, S. Young, S. J. Coles, P. N. Horton, M. E. Light and P. A. Gale, *Angew. Chem. Int. Ed.*, 2012, **51**, 4426–4430.

[19] I. Marques, P. M. R. Costa, M. Q. Miranda, N. Busschaert, E. N. W. Howe, H. J. Clarke, C. J. E. Haynes, I. L. Kirby, A. M. Rodilla, R. Pérez-Tomás, P. A. Gale and V. Félix, *Phys. Chem. Chem. Phys.*, 2018, **20**, 20796–20811.

[20] W. A. Harrell Jr, M. L. Bergmeyer, P. Y. Zavalij and J. T. Davis, *Chem. Commun.*, 2010, **46**, 3950–3952.

[21] K. M. Bąk, K. Chabuda, H. Montes, R. Quesada and M. J. Chmielewski, *Org. Biomol. Chem.*, 2018, **16**, 5188–5196.

[22] P. A. Gale, C. C. Tong, C. J. E. Haynes, O. Adeosun, D. E. Gross, E. Karnas, E. M. Sedenberg, R. Quesada and J. L. Sessler, *J. Am. Chem. Soc.*, 2010, **132**, 3240–3241.

[23] E. Hernando, V. Soto-Cerrato, S. Cortés-Arroyo, R. Pérez-Tomás and R. Quesada, *Org. Biomol. Chem.*, 2014, **12**, 1771–1778.

[24] H. Valkenier, O. Akrawi, P. Jurček, K. Sleziaková, T. Lízal, K. Bartik and V. Šindelář, *Chem*, 2019, **5**, 429–444.

[25] M. Lisbjerg, H. Valkenier, B. M. Jessen, H. Al-Kerdi, A. P. Davis and M. Pittelkow, *J. Am. Chem. Soc.*, 2015, **137**, 4948–4951.

[26] S. Chen, S. Zhang, C. Bao, C. Wang, Q. Lin and L. Zhu, *Chem. Commun.*, 2016, **52**, 13132–13135.

[27] B. Shen, X. Li, F. Wang, X. Yao and D. Yang, *PLoS ONE*, 2012, **7**, e34694.

[28] H. Li, H. Valkenier, L. W. Judd, P. R. Brotherhood, S. Hussain, J. A. Cooper, O. Jurček, H. A. Sparkes, D. N. Sheppard and A. P. Davis, *Nat. Chem.*, 2016, **8**, 24–32.

[29] E. Hernando, V. Capurro, C. Cossu, M. Fiore, M. García-Valverde, V. Soto-Cerrato, R. Pérez-Tomás, O. Moran, O. Zegarra-Moran and R. Quesada, *Sci. Rep.*, 2018, **8**, 2608.

[30] M. J. Spooner, H. Li, I. Marques, P. M. R. Costa, X. Wu, E. N. W. Howe, N. Busschaert, S. J. Moore, M. E. Light, D. N. Sheppard, V. Félix and P. A. Gale, *Chem. Sci.*, 2019, **10**, 1976–1985.

[31] H. Li, H. Valkenier, A. G. Thorne, C. M. Dias, J. A. Cooper, M. Kieffer, N. Busschaert, P. A. Gale, D. N. Sheppard and A. P. Davis, *Chem. Sci.*, 2019, **10**, 9663–9672.

32 I. Carreira-Barral, M. Mielczarek, D. Alonso-Carrillo, V. Capurro, V. Soto-Cerrato, R. P. Tomás, E. Caci, M. García-Valverde and R. Quesada, *Chem. Commun.*, 2020, **56**, 3218–3221.

33 M. Fiore, C. Cossu, V. Capurro, C. Picco, A. Ludovico, M. Mielczarek, I. Carreira-Barral, E. Caci, D. Baroni, R. Quesada and O. Moran, *J. Cystic Fibrosis*, 2019, **176**, 1764–1779.

34 D. A. Stoltz, D. K. Meyerholz and M. J. Welsh, *N. Engl. J. Med.*, 2015, **372**, 351–362.

35 A. Gianotti, V. Capurro, L. Delpiano, M. Mielczarek, M. García-Valverde, I. Carreira-Barral, A. Ludovico, M. Fiore, D. Baroni, O. Moran, R. Quesada and E. Caci, *Int. J. Mol. Sci.*, 2020, **21**, 1488.

36 K. A. Muraglia, R. S. Chorghade, B. R. Kim, X. X. Tang, V. S. Shah, A. S. Grillo, P. N. Daniels, A. G. Cioffi, P. H. Karp, L. Zhu, M. J. Welsh and M. D. Burke, *Nature*, 2019, 1.

37 A. V. Koulov, T. N. Lambert, R. Shukla, M. Jain, J. M. Boon, B. D. Smith, H. Li, D. N. Sheppard, J.-B. Joos, J. P. Clare and A. P. Davis, *Angew. Chem. Int. Ed.*, 2003, **42**, 4931–4933.

38 P.-Y. Liu, S.-T. Li, F.-F. Shen, W.-H. Ko, X.-Q. Yao and D. Yang, *Chem. Commun.*, 2016, **52**, 7380–7383.

39 S. J. Butler, *Chem. Commun.*, 2015, **51**, 10879–10882.

40 H. Valkenier, L. W. Judd, H. Li, S. Hussain, D. N. Sheppard and A. P. Davis, *J. Am. Chem. Soc.*, 2014, **136**, 12507–12512.

41 R. Sandeaux, J. Sandeaux, C. Gavach and B. Brun, *Biochim. Biophys. Acta, Biomembr.*, 1982, **684**, 127–132.

42 K. Nakazato and Y. Hatano, *Biochim. Biophys. Acta, Biomembr.*, 1991, **1064**, 103–110.

43 Y. N. Antonenko, T. I. Rokitskaya and A. Huczyński, *Biochim. Biophys. Acta, Biomembr.*, 2015, **1848**, 995–1004.

44 D. Łowicki and A. Huczyński, *Biomed Res. Int.*, 2013, **2013**, 742149.

45 C. Ho and J. M. Sturtevant, *J. Biol. Chem.*, 1963, **238**, 3499–3501.

46 A. L. Soli and R. H. Byrne, *Mar. Chem.*, 2002, **78**, 65–73.

47 V. Endeward, M. Arias-Hidalgo, S. Al-Samir and G. Gros, *Membranes*, 2017, **7**, 61.

48 P. J. F. Henderson, J. D. McGivan and J. B. Chappell, *Biochem. J.*, 1969, **111**, 521–535.

49 S. G. McLaughlin and J. P. Dilger, *Physiol. Rev.*, 1980, **60**, 825–863.

50 "Biological Buffers," in CRC Handbook of Chemistry and Physics, 100th Edition (Internet Version 2019), John R. Rumble, ed., CRC Press/Taylor & Francis, Boca Raton, FL.

51 X. Wu, L. W. Judd, E. N. W. Howe, A. M. Withecombe, V. Soto-Cerrato, H. Li, N. Busschaert, H. Valkenier, R. Pérez-Tomás, D. N. Sheppard, Y.-B. Jiang, A. P. Davis and P. A. Gale, *Chem*, 2016, **1**, 127–146.

52 T. Sato, H. Konno, Y. Tanaka, T. Kataoka, K. Nagai, H. H. Wasserman and S. Ohkuma, *J. Biol. Chem.*, 1998, **273**, 21455–21462.

53 J. L. Seganish and J. T. Davis, *Chem. Commun.*, 2005, 5781–5783.

54 Y. Yang, X. Wu, N. Busschaert, H. Furuta and P. A. Gale, *Chem. Commun.*, 2017, **53**, 9230–9233.

55 J. P. Clare, A. J. Ayling, J.-B. Joos, A. L. Sisson, G. Magro, M. N. Pérez-Payán, T. N. Lambert, R. Shukla, B. D. Smith and A. P. Davis, *J. Am. Chem. Soc.*, 2005, **127**, 10739–10746.

56 S. H. Hewitt, G. Macey, R. Mailhot, M. R. J. Elsegood, F. Duarte, A. M. Kenwright and S. J. Butler, *Chem. Sci.*, 2020, **11**, 3619–3628.

57 R. Quesada and R. Dutzler, *J. Cystic Fibrosis*, 2020, **19**, S37–S41.

58 R. Mailhot, T. Traviss-Pollard, R. Pal and S. J. Butler, *Chem. Eur. J.*, 2018, **24**, 10745–10755.